Review: Adapting Scalar Turbulence Closure Models for Rotation and Curvature

Paul Durbin
Department of Aerospace Engineering,
Iowa State University,
Ames, IA 50011
e-mail: durbin@iastate.edu

Scalar, eddy viscosity models are widely used for predicting engineering turbulent flows. System rotation, or streamline curvature, can enhance or reduce the intensity of turbulence. Methods to incorporate the effects of rotation and streamline curvature consist of introducing parametric variation of model coefficients, such that either the growth rate of turbulent energy is altered; or such that the equilibrium solution bifurcates from healthy to decaying solution branches. For general use, parameters must be developed in coordinate invariant forms. Effects of rotation and of curvature can be unified by introducing the convective derivative of the rate of strain eigenvectors as their measure.
[DOI: 10.1115/1.4004150]

1 Introduction

This review is motivated by the recent revival of interest in incorporating the influences of rotation and streamline curvature into turbulence models that are designed for practical computational fluid dynamics. Early work on this topic was formulated for nearly parallel shear flows [1,2]. Current interest is in formulations for general flows.

Practical turbulence closure models are based on transport equations for scalar variables, be they k, ε, ω, ν_T or other representative Reynolds averaged properties of the turbulent fluctuations. By their nature, scalar models do not respond appropriately to system rotation or to streamline curvature: these have their effect on individual components of the Reynolds stress tensor. A scalar formula does not distinguish components of Reynolds stress, so the correct phenomenology is not inherent in a scalar representation.

Rotation can suppress or enhance turbulence, in consequence of centrifugal acceleration in the radial direction, outward from the center of curvature. The influence in a particular direction is why a scalar model will not naturally capture such an effect. Centrifugal acceleration appears in the equations of individual Reynolds stress components but not of the overall energy.

But scalar models, especially variants of the k-ε and k-ω models, are workhorses of applied CFD [3]. The scalar variables are used to construct an eddy viscosity for mean flow prediction. How can such models be sensitized to rotation? The following reviews some primary concepts; it is not a bibliographic review.

2 Phenomonology

The basic phenomenon of streamline curvature is that convex curvature reduces turbulent intensity and concave curvature enhances it. The term "convex" refers to a boundary layer along a wall with the center of curvature inside the surface; e.g., the outside of a circular arc. The boundary layer profile is a velocity that increases radially outward from the center of curvature. A *concave* wall curves oppositely, and the velocity increases toward the center of curvature.

To characterize the effect of curvature on a shear flow, two sorts of rotation must be considered. Firstly, as the flow proceeds along a streamline over a curved wall, the direction of the velocity vector rotates. Secondly, fluid elements within a shear flow also rotate: they rotate clockwise if $dU/dy > 0$. The effect of curvature on turbulence is determined by these two direction of rotation: along a convex wall, the velocity vector rotates in the same direction as fluid elements; along a concave wall the rotations are in opposite directions. Co-rotation suppresses turbulence, counter-rotation enhances it.

An analogy exists between system rotation and streamline curvature. Think of an apparatus on a turntable. A shear flow is established in the rotating frame. If the geometry is rotating in the same direction as the shear, turbulent intensity is reduced by rotation, if they are opposite turbulent intensity increases.

Consider some examples. First, a simple, uniform shear, $U = yd_yU$ where d_yU is a constant. Without rotation, turbulent kinetic energy, k, is produced by the mean shear and k grows with time. Rotation either can enhance or reduce the growth rate, depending on whether it is against or with the shear. This is illustrated by Fig. 1 [4]. The squares show the evolution of k in nonrotating flow: note that the energy grows with time; rotation will increase or decrease that growth rate. The circles are for rotation against the shear; growth is enhanced. The triangles are for rotation with the shear, which reduces growth.

Another, commonly cited example is rotating plane channel flow [5,6,7]. The direction of shear next to one wall is opposite to that next to the other wall; so, if the channel is rotated the effect will be to enhance turbulence next to one wall and reduce it next to the other. The flow develops an asymmetry, as in Fig. 2. Here the shear next to the upper wall rotates fluid elements in the direction opposite to the frame rotation; this is the unstable side. The surface shear stress is increased on the unstable side; on the stable wall the stress drops: see Fig. 3. This effect would not be captured by native scalar, eddy viscosity models models: they are insensitive to rotation, and predict the flow to remain symmetric about the channel centerline.

Other, fundamental examples appear in the literature. Effects of curvature are seen in a U-shaped channel, where the inner wall is convex and the outer wall is concave [8]. The vortex street downstream of a circular cylinder in a rotating apparatus becomes asymmetric, as the vortices either co-rotate or counter-rotate with the reference frame [9]. Similarly, separation bubbles elongate with co-rotation because of the reduction of turbulent mixing and shrink under counter rotation. Benchmark data on this phenomenon have been obtained in flow over a backward facing step [10,11] and in a serpentine duct [12]. Other examples can be found in [13].

A simple stability argument illustrates the concept. Set the x derivatives to zero in the equations for a linear perturbation of homogeneous shear, $U = yd_yU$. In a rotating frame Coriolis acceleration is included, and the equations are

$$\frac{du}{dt} = 2\Omega^F v - d_yUv$$
$$\frac{dv}{dt} = 2\Omega^F u \tag{1}$$

Contributed by the Fluids Engineering Division of ASME for publication in the JOURNAL OF FLUIDS ENGINEERING. Manuscript received December 13, 2010; final manuscript received April 22, 2011; published online June 16, 2011. Assoc. Editor: Malcolm J. Andrews.

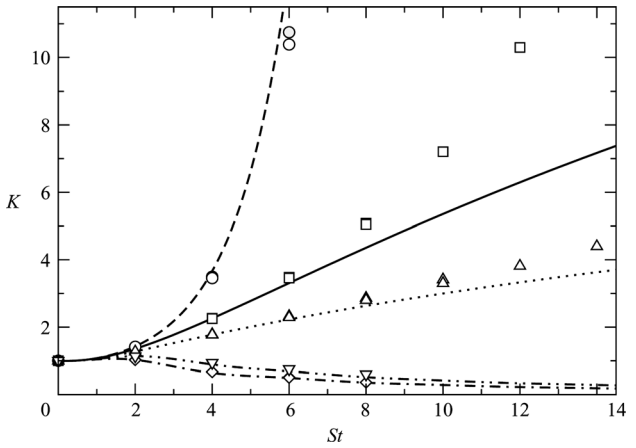

Fig. 1 Evolution of k with time for ○, $Ro = -1/2$; □, $Ro = 0$; Δ, $Ro = -1$; ◇, $Ro = -3/2$; ∇, $Ro = 1/2$. The symbols are from DNS, the curves from rapid distortion theory. From Ref. [4].

The pressure drops out because the disturbance is elongated in the streamwise direction; $\partial_x = 0$. Combining Eq. (1) and defining the rotation parameter

$$Ro = -2\Omega^F / d_y U \tag{2}$$

gives

$$\frac{d^2u}{dt^2} = -Ro(Ro+1)d_y U^2 u \tag{3}$$

The general solution is $u = \exp(\pm\sqrt{-Ro(Ro+1)}d_y U t)$. So if $-1 < Ro < 0$ the exponent is real and one solution grows exponentially in time. If $Ro = 0$ or -1 the solution is $u = u_0 + \dot{u}_0 t$, which suggests that the solution is still growing, although no longer exponentially; indeed, $Ro = 0$ is (homogeneous) shear without rotation, for which the turbulent energy does grow.

Figure 1 shows the evolution of turbulent kinetic energy with time for unstable ($Ro = -1, -1/2, 0$) and stable cases ($Ro = -3/2, 1/2$). In the unstable cases, energy grows with time; in the stable cases it decays. The most rapid growth is for $Ro \approx -1/2$.

The range of growing turbulence is a bit wider than $-1 < Ro < 0$; say, $Ro_{s2} < Ro < Ro_{s1}$ where Ro_{s2} and Ro_{s1} are empirical, but not far from -1 and 0. Stabilization when $Ro > Ro_{s1}$ corresponds to turbulence being suppressed by frame rotation in the same direction as the shear. Rotation against the shear $Ro < 0$ is initially destabilizing, but if it is sufficiently strong, $Ro < Ro_{s2}$, it becomes stabilizing.

The factor of $-Ro(Ro+1)$ gives maximum growth at $Ro = -1/2$, consistent with Fig. 1; but it gives a growth rate that is symmetric about $Ro = -1/2$, which is not correct; growth rates at $Ro = 0$ and $Ro = -1$ differ. Ignoring pressure and viscosity in

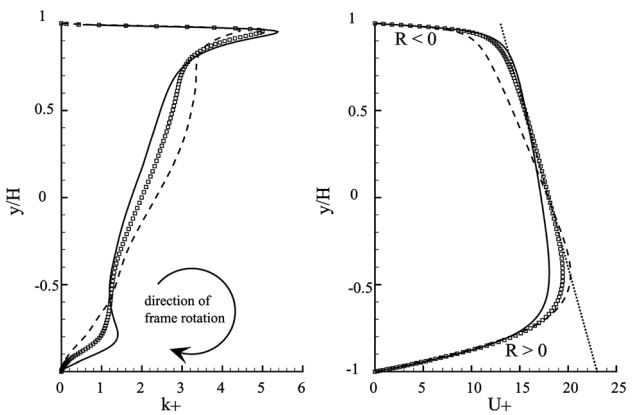

Fig. 2 Turbulent kinetic energy and mean flow for rotating channel; curves for three rotation rates. From Ref. [5]

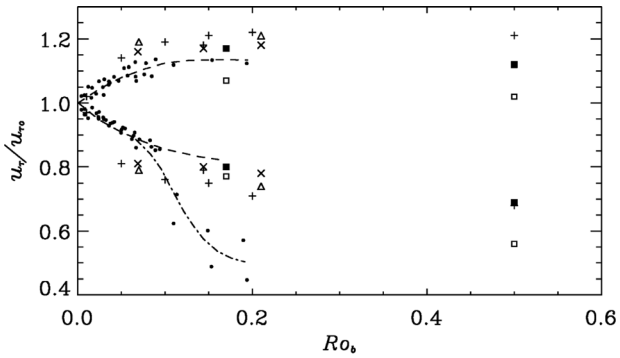

Fig. 3

(1) is overly simplistic; nevertheless, some quick insights do accrue from the present analysis. Reformulated as Reynolds stress evolution equations, (1) becomes

$$\begin{aligned}
\frac{1}{2}\frac{\overline{du^2}}{d\tau} &= -\overline{uv}(Ro+1) \\
\frac{1}{2}\frac{\overline{dv^2}}{d\tau} &= -\overline{uv}Ro \\
\frac{\overline{duv}}{d\tau} &= -\overline{v^2} + Ro\left(\overline{u^2} - \overline{v^2}\right)
\end{aligned} \tag{4}$$

where $\tau = d_y U t$. These equations show that rotation does not directly affect the growth of kinetic energy (cf., $\overline{u^2} + \overline{v^2}$) and that rotation creates anisotropy (cf., $\overline{u^2} - \overline{v^2}$). Anisotropy affects the shear stress, and thereby alters the production of turbulent energy, k. The dilemma of two-equation closure modeling is that the effect of Ro on k is indirect.

3 Equilibria of the K and ε Equations

Analysis of moving equilibria is a key method in turbulence modeling. Consider the standard k-ε equations in homogeneous turbulence:

$$\begin{aligned}
\frac{dk}{dt} &= \mathcal{P} - e \\
\frac{d\varepsilon}{dt} &= \frac{C_{\varepsilon 1}\mathcal{P} - C_{\varepsilon 2}P}{\mathrm{T}}
\end{aligned} \tag{5}$$

where $T = k/\varepsilon$ is the turbulent time-scale and

$$\mathcal{P} = -\overline{u_i u_j} S_{ji} \tag{6}$$

is the rate of energy production. S_{ji} is the rate of strain tensor [see Eq. (23)].

Following [14], Eq. (5) can be combined into

$$\frac{d}{dt}\left(\frac{\varepsilon}{k}\right) = \left(\frac{\varepsilon}{k}\right)^2 \left[(C_{\varepsilon 1} - 1)\frac{\mathcal{P}}{\varepsilon} - (C_{\varepsilon 2} - 1)\right] \tag{7}$$

This describes two equilibria, obtained by setting $d_t(\varepsilon/k) = 0$ on the left side; they are

$$\text{branch 1:}\quad \frac{\mathcal{P}}{\varepsilon} = \frac{C_{\varepsilon 2} - 1}{C_{\varepsilon 1} - 1} \tag{8a}$$

and

$$\text{branch 2:}\quad \frac{\varepsilon}{k} = 0 \tag{8b}$$

With standard values of $C_{\varepsilon 2} = 1.92$ and $C_{\varepsilon 1} = 1.44$, $\mathcal{P}/\varepsilon = 2.1$ on branch 1; or sometimes $C_{\varepsilon 2}$ is equated to 1.85 giving $\mathcal{P}/\varepsilon = 1.9$. In general, the constants give $\mathcal{P}/\varepsilon > 1$ and the k grows with time.

The equilibria (8) can be called the "healthy" and "decaying" solutions. On the healthy branch (8*a*) turbulent energy grows exponentially in time. Equation (5) have a solution of the form [3,14]

$$\text{branch 1:} \quad k = k_\infty e^{\lambda t}, \quad \varepsilon = \varepsilon_\infty e^{\lambda t} \tag{9}$$

The subscript ∞ denotes the equilibrium value, following any initial transients. Substituting these and expression (8*a*) into Eq. (5) gives

$$\lambda = \frac{C_{\varepsilon 2} - C_{\varepsilon 1}}{C_{\varepsilon 1} - 1} \left(\frac{\varepsilon}{k}\right)_\infty \tag{10}$$

A constitutive model is needed to close (6). The eddy viscosity constitutive model is

$$\overline{u_i u_j} = -2\nu_T S_{ij} + 2/3\ \delta_{ij} k \tag{11}$$

With this, the rate of energy production becomes

$$\mathcal{P} = 2\nu_T |S|^2 \tag{12}$$

where $|S|^2 = S_{ij}S_{ji}$. (Incompressibility, $S_{kk} = 0$, is assumed.) The k-ε eddy viscosity is $\nu_T = C_\mu k^2/\varepsilon$. Hence

$$\frac{\mathcal{P}}{\varepsilon} = 2C_\mu |S|^2 \left(\frac{k}{\varepsilon}\right)^2 \tag{13}$$

Substituting (8*a*) gives the equilibrium value

$$\left(\frac{\varepsilon}{|S|k}\right)_\infty = \sqrt{2C_\mu}\sqrt{\frac{C_{\varepsilon 1} - 1}{C_{\varepsilon 2} - 1}} \tag{14}$$

Then the growth exponent in (10) is

$$\lambda = \frac{C_{\varepsilon 2} - C_{\varepsilon 1}}{\sqrt{(C_{\varepsilon 1} - 1)(C_{\varepsilon 2} - 1)}} \sqrt{2C_\mu |S|^2} \tag{15}$$

Once the scalar eddy viscosity assumption is adopted, this solution is unaltered by rotation. In parallel shear flow $2|S|^2 = |\partial_y U|^2$.

The solution on the second branch (8*b*) has the power law form [3]

$$\text{branch 2:} \quad k = A_\infty t^m, \varepsilon = B_\infty t^{m-1} \tag{16}$$

Thus $\varepsilon/k \propto 1/t \to 0$ as $t \to \infty$. Substituting these into the k and ε-equations (5) gives

$$m = \frac{\mathcal{P}/\varepsilon - 1}{(C_{\varepsilon 2} - 1) - P/\varepsilon(C_{\varepsilon 1} - 1)} \tag{17}$$

If $\mathcal{P} < \varepsilon$ the exponent m is negative and turbulent energy decays; that is $d_t k < 0$ in (5). There is a range $1 < \mathcal{P}/\varepsilon < (C_{\varepsilon 2} - 1)/(C_{\varepsilon 1} - 1)$ where m is positive. For the standard values $C_{\varepsilon 2} = 1.92$ and $C_{\varepsilon 1} = 1.44$ this range is $1 < \mathcal{P}/\varepsilon < 2.1$. In that range k grows algebraically. When $\mathcal{P} < \varepsilon$, k decays algebraically.

Stabilization when $Ro > Ro_{s1}$ means that $\mathcal{P}/\varepsilon$ is reduced below unity. How can this occur within a scalar, eddy viscosity assumption? Can rotation stabilize the solution? The answer is obvious: rotation does not appear in the equations of the k-ε model; so, no.

The equilibrium solution to many Reynolds stress transport models can be stated in the form but C_μ is replaced by a function that depends on Ω^F [3,16]. That function is such that the right side of (14) becomes zero at two values of Ro: for the IP model they are -0.750 and 0.178; for the SSG [17] model they are -1.05 and 0.159. (The SSG model was designed to make these close to -1 and 0). Outside the interval between the zeros, ε/k is would be imaginary on branch 1; thus, the real solution moves to branch 2. The term *bifurcation* is used to describe this behavior.

The mathematics of Reynolds stress models is complex [3], but quite attractive: the transition from the healthy to the decaying solution branch captures the phenomenology. The physics derive from suppression of individual components of Reynolds stress by rotation. Either full Reynolds stress transport models, or algebraic tensor models retain those effects [16]. However, a less physical, pragmatic approach also can be discussed within the framework of the equilibrium analysis.

4 Modified Coefficients

It has been proposed in the literature, as an operational device, that the coefficients of the $k - \varepsilon$ (or $k - \omega$) model be given a parametric dependence on the rotation number

$$Ro \equiv -2\Omega^F/\partial_y U \tag{18}$$

so as to cause stabilization. An ad hoc approach would be to make them functions of rates of rotation and strain, such that the growth rate (10) becomes negative in stable regions. According to (8*a*) $\mathcal{P}/\varepsilon = 1$ if $C_{\varepsilon 2} = C_{\varepsilon 1}$. Either $C_{\varepsilon 2}$, $C_{\varepsilon 1}$ or both could vary to reduce $\mathcal{P}/\varepsilon$ below unity. Then the growth rate, λ in (10), would become negative. Various proposals for adapting $C_{\varepsilon 2}$ to this end will be reviewed.

The Bradshaw [18] parameter

$$Br = Ro(Ro + 1) \tag{19}$$

arose in the stability analysis [Eq. (3)]. $Br < 0$ is the unstable range. Note that Br is symmetric about $Ro = -1/2$ and has the minimum value of $-1/4$. Although that symmetry is not exactly respected by turbulence dynamics—see Fig. 1—Br has been used for parametric modeling. An empirical definition

$$Br = (Ro - Ro_1)(Ro - Ro_2)$$

might be better suited to the data. Second moment closure models give stabilization points of about $Ro_1 \sim 0.18$ and $Ro_2 \sim -1.07$: then $Br = -0.19$ when $Ro = 0$ and $Br = -0.083$ when $Ro = -1$, consistent with the latter having a lower growth rate than the former. Br is minimum at $Ro = (Ro_1 + Ro_2)/2$.

Rather than accepting the linear result of $Ro > 0$ for stability, a critical value, Br_{crit}, above which rotation suppresses turbulence can be postulated. An early proposal to model rotational stabilization was [2]

$$C_{\varepsilon 2} = C^0_{\varepsilon 2}(1 - C_{sc} Br) \tag{20}$$

Then by (8*a*) $\mathcal{P}/\varepsilon$ becomes unity at the critical value found from

$$C_{\varepsilon 1} = C_{\varepsilon 2} = C^0_{\varepsilon 2}(1 - C_{sc} Br_{\text{crit}})$$

or

$$Br_{\text{crit}} = \frac{C^0_{\varepsilon 2} - C_{\varepsilon 1}}{C^0_{\varepsilon 2} C_{SC}}$$

For the standard k-ε constants ($C^0_{\varepsilon 2} = 1.92$ and $C_{\varepsilon 1} = 1.44$, so that $C^0_{\varepsilon 2} = (4/3)C_{\varepsilon 1}$) this is $1/4C_{sc}$. With $C_{sc} = 2.5$ the critical Bradshaw number becomes 0.1. With that value, the exponent λ becomes negative when $Br > 0.1$; or equivalently, when $R > 0.09$ or $R < -1.1$.

A similarly simple proposal was made by [19] for the $k\omega$-model: $C_{\omega 2} = C^0_{\omega 2}/(1 + C_{sc} Br)$. Translated into $k - \varepsilon$ (that is, $C_{\varepsilon 2} = 1 + C_{\omega 2}$) it is

$$C_{\varepsilon 2} = \frac{C^0_{\varepsilon 2} + C_{SC} Br}{1 + C_{SC} Br} \tag{21}$$

This gives

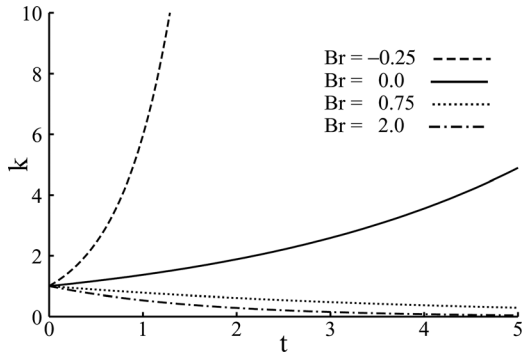

Fig. 4 Turbulent kinetic energy in rotating homogeneous shear by 2-equation model with (21)

$$Br_{\text{crit}} = \frac{C^0_{\varepsilon 2} - C_{\varepsilon 1}}{(C_{\varepsilon 1} - 1)C_{SC}} = \frac{12}{11C_{SC}}$$

With the recommended value $C_{cs} = 3.6$ this becomes $Br_{crit} = 0.30$, corresponding to $Ro = -1.24$ and 0.24. Note that the minimum value $Br = -1/4$ gives a finite, although quite large, value of 10.2 for $C_{\varepsilon 2}$. Figure 4 illustrates the behavior of this model. k is normalized by its initial value, time is normalized by $|\mathbf{S}|$, and ε is initialized to the equilibrium value (14). k grows far too fast when $Br = -0.25$. This model is illustrated for rotating channel flow in Fig. 5; in this case, it shows too little sensitivity to rotation.

The curves in Fig. 4 are just exponentials, with λ given by (15). For an arbitrary initial condition there will be a transient, evolving asymptotically to exponential growth or decay. One must be careful to distinguish the rotation model from the influence of initial conditions; for example, if ε initially is small, a solution with $Ro = 0.5$ might first grow, and then decay. Model development is guided by the equilibrium solution, which is approached after initial transients.

The definition (18) of Ro becomes infinite where the shear vanishes, such as in the center of channel flow. Hence, some proposals are parameterized by

$$Br \times (|\mathbf{S}|k/\varepsilon)^2$$

However, this can lead to spurious behavior [20]. As an example, consider

$$C_{\varepsilon 2} = C^0_{\varepsilon 2}(1 - C_{sc}Br(|\mathbf{S}|k/\varepsilon)^2) \tag{22}$$

with $C_{sc} = 0.4$, which [20] calls the HPB model [21]. Invoking the equilibrium solution (14) and solving for $C_{\varepsilon 2}$ gives

$$C_{\varepsilon 2} = \frac{C^0_{\varepsilon 2} + ABr}{1 + ABr}; \quad A = \frac{C_{SC}C^0_{\varepsilon 2}}{2C_\mu(C_{\varepsilon 1} - 1)}$$

With the standard constants, $A = 9.7$. Equating this formula to $C_{\varepsilon 1}$ gives the critical value

$$Br_{\text{crit}} = \frac{C^0_{\varepsilon 2} - C_{\varepsilon 1}}{A(C_{\varepsilon 1} - 1)} = 0.026$$

The HPB model behaves well near the critical Bradshaw number, but if $C_{\varepsilon 2} < 1$ the solution (14) is imaginary. In fact $C_{\varepsilon 2}$ becomes negative for

$$Br < -1/A = -0.103$$

Since the minimum value of Br is -0.25, there is a range of rotation rates where the model is ill posed. The form $C_{\varepsilon 2} = C^0_{\varepsilon 2}/(1 + C_{sc}Br(|\mathbf{S}|k/\varepsilon)^2)$ would avoid the singularity.

Cazalbou [20] proposed a functional dependence that is not ill posed. It is somewhat involved and the reader is referred to the original paper for details.

Another idea would be to make $C_{\varepsilon 2}$ *increase* with rotation, consistent with observations of the decay exponent for grid turbulence [23]. The coefficient $C_{\varepsilon 2}$ is related to the decay exponent in grid turbulence, $k \sim t^{-n}$, by $C_{\varepsilon 2} = 1 + 1/n$. The non-rotating value is $n \approx 1.2$. Under strong rotation n decreases, approaching 0.6 [24]. Since that is opposite to the change needed to stabilize the turbulence, stabilization could be introduced by making $C_{\varepsilon 1}$ a function of Br. To date this has not been pursued.

In the context of a one-equation, eddy viscosity transport model, Spalart and Shur [25,26] defined a parameter that is equivalent to the inner product of vorticity and the rotation vector: $\boldsymbol{\omega} \cdot \boldsymbol{\omega}^F$—actually, they introduced an important generalization of frame rotation that will be described below. They added an ad hoc function into an eddy viscosity transport equation in order to enhance or reduce production, depending on the sign of this inner product. In homogeneous turbulence the transport equation contains only a production term, so this approach is inescapable. It, too, is like altering the growth exponent λ.

4.1 Invariant Form of Rotation Parameter. The definition (2) of the rotation parameter is only suited to parallel flow, rotating about an axis perpendicular to the plane of the flow. That is not sufficiently general for use in CFD. The rotation parameter must be defined in terms of invariants of the velocity gradient.

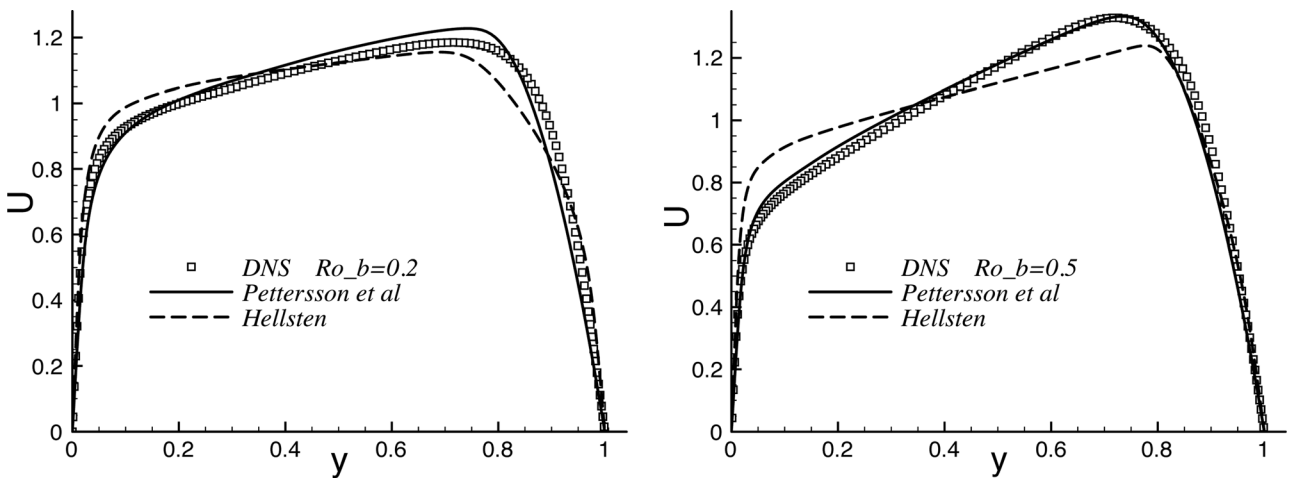

Fig. 5 Mean velocity in channel with bulk rotation numbers $Ro_b = 2\Omega^F/U_b = 0.2$ and 0.5. Symbols are DNS data of Ref. [5]; models are from Refs. [19] and [22]

The rate of strain and rate of rotation are

$$S_{ij} \equiv \frac{1}{2}\left(\partial_j U_i + \partial_i U_j\right)$$
$$\Omega^A_{ij} \equiv \frac{1}{2}\left(\partial_i U_j - \partial_j U_i\right) \tag{23}$$

The superscript on Ω^A indicates that this is the absolute rotation, relative to an inertial frame. Relative to a frame rotating with angular velocity vector ω^F_i

$$\Omega^A_{ij} = \frac{1}{2}\left(\partial_i U^{\text{rel}}_j - \partial_j U^{\text{rel}}_i\right) + \varepsilon_{ijk}\omega^F_k \equiv \Omega^{\text{rel}}_{ij} + \Omega^F_{ij} \tag{24}$$

Define the magnitudes

$$|\mathbf{S}|^2 = S_{ij}S_{ij} = \text{trace}(\mathbf{S}^2) \quad \text{and} \quad |\mathbf{\Omega}|^2 = \Omega_{ij}\Omega_{ij} = -\text{trace}(\mathbf{\Omega}^2)$$

(Beware that some references add a factor of 2 on the right side and note that the trace of the square of an anti-symmetric tensor is negative.) Khodak and Hirsh [27] suggest replacing frame rotation by $|\mathbf{\Omega}^A| - |\mathbf{S}|$. The Bradshaw number (19) is redefined by the invariant form

$$Br = \frac{|\mathbf{\Omega}^A|(|\mathbf{\Omega}^A| - |\mathbf{S}|)}{|\mathbf{S}|^2} \tag{25}$$

In parallel shear flow $|\mathbf{\Omega}^A| = |\Omega^F - (1/2)\partial_y U|$ and $|\mathbf{S}|^2 = (1/2)|\partial_y U|^2$. Then this definition becomes

$$Br = |Ro + 1|(|Ro + 1| - 1)$$

and for $|Ro| \le 1$ it is the same as definition (19).

4.2 Bifurcation. If one interprets the modified coefficient approach of Sec. 4 in physical terms, the mechanism is that rotation increases the dissipation rate until $\mathcal{P} < \varepsilon$. That is the consequence of decreasing $C_{\varepsilon 2}$. But it is not correct: the actual physical mechanism is that centrifugal stabilization suppresses the production of turbulence. Indeed, that is how the inviscid stability analysis [Eq. (3)] describes it—and how the Reynolds stress transport equations describe it as well. Generally $C_{\varepsilon 2}$ retains a constant value.

To repeat another criticism of the models described in the previous section: full second moment models are not parameterized by Br. Figure 1 illustrates this. $Ro = 0$ and $Ro = -1$ both give $Br = 0$, but the evolution of k differs. The stable cases, $Ro = 0.5$ and $Ro = -1.5$, both have $Br = 0.75$ and evolve somewhat similarly.

To this point we have not made use of the branch 2 solution (8b). Equilibrium analysis of second moment closure models shows how branch 1 [Eq. (8)] ceases to exist when the rotation rate is above one limit, or below another—corresponding approximately to $Ro > 0$ or $Ro < -1$. In those ranges the equilibrium shifts to the branch 2 solution. The term *bifurcation* refers to this behavior. How can this be utilized in scalar models?

It can be introduced into two-equation models by making C_μ depend on the rate of strain and rate of rotation [22,28,29]. In particular let

$$S_{ij} \equiv \frac{1}{2}\left(\partial_j U_i + \partial_i U_j\right)$$
$$\Omega^*_{ij} = \Omega^{\text{rel}}_{ij} + C_r\varepsilon_{ijk}\omega^F_k = \Omega^{\text{rel}}_{ij} + C_r\Omega^F_{ij} \tag{26}$$

where C_r is a model constant, and define

$$\eta_1 = S_{ij}S_{ij}(k/\varepsilon)^2 = |\mathbf{S}k/\varepsilon|^2$$
$$\eta_2 = \Omega^*_{ij}\Omega^*_{ij}(k/\varepsilon)^2 = |\mathbf{\Omega}^* k/\varepsilon|^2 \tag{27}$$

The eddy viscosity formula (13) is

$$\frac{\mathcal{P}}{\varepsilon} = 2C_\mu\eta_1 \tag{28}$$

Let $C_\mu = F_\mu(\eta_1, \eta_2/\eta_1)$. The argument η_2/η_1 is a generalization of the rotation parameter. Then on branch 1

$$\frac{C_{\varepsilon 2} - 1}{C_{\varepsilon 1} - 1} = 2\eta_1 F_\mu \tag{29}$$

The left side is a constant, so this defines a curve $\eta_1 = fcn(\eta_2/\eta_1)$. Examples are shown in Fig. 6: the vertical axis is $1/\sqrt{\eta_1}$.

In rotating parallel shear flow η_2/η_1 becomes $(1 + C_r Ro)^2$. A suitable constant is $C_r = 2.25$ [22]. In Fig. 6 the horizontal axis is $1 + C_r Ro$. The curves hit $1/\eta_1 = 0$ for $Ro \sim -1.07$ and $Ro \sim 0.18$. Beyond these values (29) would require η_1 to be negative. That is impossible [by definition (27)] so branch 1 ceases to exist. The equilibrium solution moves to branch 2, where $1/\eta_1 = 0$. Then the formula (28) is used to find $\mathcal{P}/\varepsilon$ by taking the limit $\eta_1 \to \infty$:

$$\frac{\mathcal{P}}{\varepsilon} = \lim_{\eta_1 \to \infty}(2F_\mu\eta_1) \tag{30}$$

This is a constraint on the possible forms of F_μ: the right side must be a finite valued function of η_2/η_1 [30]. Another way to describe this condition is that the model can bifurcate only if there are Ro such that $F_\mu(Ro) = 0$; these are the bifurcation points.

As an example let F_μ have the form

$$F_\mu = \frac{C_\mu}{1 + \eta_1 A[1 - G(\eta_2/\eta_1)]} \tag{31}$$

in which $A = 2C_\mu(C_{\varepsilon 1} - 1)/(C_{\varepsilon 2} - 1)$. Equation (29) gives

$$\frac{1}{\eta_1} = \frac{A}{C_\mu}F_\mu = \frac{A}{1 + \eta_1 A[1 - G(\eta_2/\eta_1)]}$$

Solving this,

$$\frac{1}{\eta_1} = AG(\eta_2/\eta_1)$$

Thus G has the shape of the curves in Fig. 6. Branch 1 is the range in which $G > 0$. The bifurcation points are the zeros of G. By definition $\eta_1 > 0$ so branch 1 disappears when $G < 0$.

The SSG bifurcation curve in Fig. 6 suggests a form

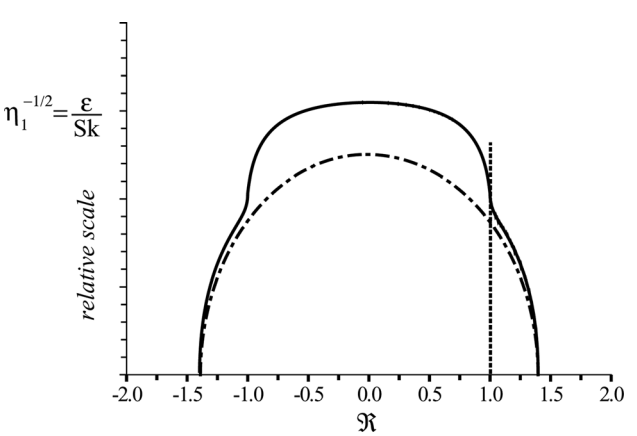

Fig. 6 Bifurcation diagram. Two examples: chaindash curve is the SSG solution, solid is from Ref. [22]. $\Re = \sqrt{\eta_2/\eta_1} = 1 + C_r Ro$. The vertical line at $\Re = 1$ is the non-rotating case.

$$G = \frac{1.85 - (\eta_2/\eta_1)}{|1.45 - 0.6(\eta_2/\eta_1)|} \tag{32}$$

For parallel shear flow $\eta_2/\eta_1 = (1 + C_r Ro)^2$ and the bifurcation points, $\eta_2/\eta_1 = 1.85$, are at $Ro = (\pm 1.36 - 1)/C_r$. Using the value $C_r = 2.25$ gives $Ro_{b1} = 0.16$ and $Ro_{b2} = -1.04$.

In fact the formula (32) was constrained to reproduce these bifurcation points. It also was constrained to become unity when $Ro = 0$; that is, when $\eta_2 = \eta_1$. This ensures that the model is unchanged in non-rotating flow.

On branch 2 the decay exponent (17) is found after evaluating (30):

$$\frac{\mathcal{P}}{\varepsilon} = \lim_{\eta_1 \to \infty} \frac{\eta_1 C_\mu}{1 + \eta_1 A(1 - G)} = \frac{C_{\varepsilon 2} - 1}{(C_{\varepsilon 1} - 1)(1 - G)}$$

On this branch $G < 0$ and is a decreasing function of rotation. Thus, $\mathcal{P}/\varepsilon$ decreases, dropping below unity at some rotation rate; for (32) $\mathcal{P}/\varepsilon$ equals unity at $\eta_2/\eta_1 = 2.11$ or $Ro = 0.20$ and $Ro = -1.09$. After that turbulence decays. So bifurcation is not synonymous with the onset of decay; rather it commences where $\mathcal{P} = \varepsilon$.

The illustrative formula (32) for G becomes infinite at $\eta_2/\eta_1 = 1.45/0.6$ but the denominator could be bounded from below: $\max(1.45 - 0.6\eta_2/\eta_1, \delta)$. Limiters are not uncommon in applied turbulence modeling. Applications of this method to the v^2-f and k-ω models are presented in Refs. [22] and [28]; these articles contain formulas alternative to (32). An example using the formulation of Ref. [22] is included in Fig. 5.

5 Unification of Rotation and Streamline Curvature

Early ideas about incorporating streamline curvature were based on exact metric terms in the Reynolds stress transport equations [1]. Metrics express curvature of the coordinate system, not of the streamlines, but in thin, 2-D shear flows they can be nearly the same. More generally, the tangent to the streamline is $\mathbf{t} = \mathbf{U}/|\mathbf{U}|$ and the curvature is $|(\mathbf{t} \cdot \nabla)\mathbf{t}|$. However, streamlines are not Galilean invariant; for that reason Girimaji [31] suggested to replace $\mathbf{U}$ by $D\mathbf{U}/Dt$, calling this the acceleration coordinate system. However, Hellsten [32] showed that the curvature of the acceleration system can grossly over estimate the correct, metric, curvature. Such efforts to obtain a literal version of streamline curvature have been supplanted by a method that unifies rotation and curvature via the convective derivative of the rate of strain tensor.

The rate of strain tensor can be expressed as

$$\mathbf{S} = \sum_{\alpha=1}^{3} \lambda_\alpha \mathbf{e}^\alpha \mathbf{e}^\alpha \tag{33}$$

The $\mathbf{e}$'s are unit eigenvectors and the λ's are eigenvalues. Unit vectors can only change by rotating,

$$D_t \mathbf{e}^\alpha = \Omega^S_{\alpha\beta} \mathbf{e}^\beta$$

In other words, the axes rotate at a rate

$$\Omega^S_{\alpha\beta} = D_t \mathbf{e}^\alpha \cdot \mathbf{e}^\beta \tag{34}$$

This is the most direct definition of Ω^S. During a computation, the eigenvectors of the rate of strain tensor must be evaluated at each time step and at every grid point. Then their convective derivative can be computed. The eigenvector evaluations can be computationally expensive.

Before proceeding to other methods of evaluating Ω^S, where it enters modeling should be mentioned. It is quite straightforward: the models that were described in previous sections to represent frame rotation are revised by replacing Ω^F in definitions (26) and (24) by Ω^S. Thereby they are made sensitive to curvature by invoking the analogy between curvature and rotation [18]. [If Ω^S were evaluated relative to a rotating frame, $\boldsymbol{\omega}^F$ would be added on the right side (34)].

Spalart and Shur [25] propose, on the grounds of computational efficiency, to replace the eigenvectors on the right side of Eq. (34) by the full rate of strain tensor. First, instead of $D_t \mathbf{e}^\alpha$, consider the convective derivative of the rate of strain tensor (33):

$$\begin{aligned} D_t \mathbf{S} &= \mathbf{e}^\alpha \mathbf{e}^\alpha D_t \lambda_\alpha + \lambda_a [\mathbf{e}^\alpha D_t \mathbf{e}^\alpha + (D_t \mathbf{e}^\alpha)\mathbf{e}^\alpha] \\ &= \mathbf{e}^\alpha \mathbf{e}^\alpha D_t \lambda_\alpha + \lambda_\alpha \mathbf{e}^\alpha \mathbf{e}^\beta \Omega^S_{\alpha\beta} + \Omega^S_{\alpha\beta} \mathbf{e}^\beta \mathbf{e}^\alpha \lambda_\alpha \\ &= \text{Diag} + (\lambda_\alpha \mathbf{e}^\alpha \mathbf{e}^\alpha) \cdot \left(\mathbf{e}^\alpha \mathbf{e}^\beta \Omega^S_{\alpha\beta}\right) - \left(\Omega^S_{\beta\alpha} \mathbf{e}^\beta \mathbf{e}^\alpha\right) \cdot (\lambda_\alpha \mathbf{e}^\alpha \mathbf{e}^\alpha) \\ &= \text{Diag} + \mathbf{S} \cdot \boldsymbol{\Omega}^S - \boldsymbol{\Omega}^S \cdot \mathbf{S} \end{aligned} \tag{35}$$

(with implied summation over α and β) in which Diag is a symmetric tensor. Next construct an analogy to (34). $D_t \mathbf{S}$ is symmetric, but an anti-symmetric tensor can be created as

$$\mathbf{W} \equiv \frac{\mathbf{S} \cdot D_t \mathbf{S} - D_t \mathbf{S} \cdot \mathbf{S}}{2|\mathbf{S}|^2} \tag{36}$$

This uses the property that the product of symmetric tensors is not necessarily symmetric, and extracts its anti-symmetric part. We will call $\mathbf{W}$ the *Spalart-Shur tensor*.

In two-dimensions (36) can be written in terms of the components of the rate of strain tensor as

$$\mathbf{W} = \frac{S_{11} D_t S_{21} - S_{12} D_t S_{11}}{2(S_{11}^2 + S_{12}^2)} \begin{pmatrix} 0 & 1 \\ -1 & 0 \end{pmatrix} \tag{37}$$

As an example, a steady, pure strain in a rotating frame has the form

$$\mathbf{S} = \sigma \begin{pmatrix} \cos^2 \Omega t - \sin^2 \Omega t & -2 \cos \Omega t \sin \Omega t \\ -2 \cos \Omega t \sin \Omega t & \sin^2 \Omega t - \cos^2 \Omega t \end{pmatrix}$$

The reader can verify that $\boldsymbol{W}$ is the rotation matrix $\Omega \varepsilon_{ij3}$.

Upon substituting the last line of (35) into (36) the relation

$$\mathbf{W} = \frac{\mathbf{S}^2 \cdot \boldsymbol{\Omega}^S + \boldsymbol{\Omega}^S \cdot \mathbf{S}^2 - 2\mathbf{S} \cdot \boldsymbol{\Omega}^S \cdot \mathbf{S}}{2|\mathbf{S}|^2} \tag{38}$$

between the Spalart-Shur tensor, $\mathbf{W}$, and the rotation of the rate-of-strain axes is found. Assume incompressibility, or that $\mathbf{S}$ is trace free. In two dimensional flow $\mathbf{S} = \lambda \text{Diag}\,(1, -1, 0)$ and (38) becomes $\mathbf{W} = \boldsymbol{\Omega}^S$ so (37) provides the rate of rotation of the principal axes in two-dimensional flow, which could as easily have been found from (34).

For the general, three-dimensional case, the matrix Eq. (38) is a system of 3 equations for Ω^S_{12}, Ω^S_{13} and Ω^S_{23} given W_{12}, W_{13} and W_{23}. Wallin and Johansson [33] note that if rotation vectors are introduced via $w_i = (1/2)\varepsilon_{ijk} W_{jk}$ and $\Omega^S_{ij} = \varepsilon_{ijk} \omega^S_k$, then the set of three equations becomes

$$w_i = \omega^S_i - \frac{3\mathbf{S}^2_{ij}}{2|\mathbf{S}|^2} \omega^S_j \tag{39}$$

In two dimensions $\mathbf{S}^2/|\mathbf{S}|^2$ equals $(1/2)\text{diag}(1, 1, 0)$ and $\omega^S = (0, 0, \omega^S_3)$ so, again, $\mathbf{w} = \boldsymbol{\omega}^S$. The matrix on the right of (39) can be inverted via the Cayley-Hamilton theorem [33], or solved numerically as a set of three simultaneous equations.

Reverting to matrix form (39) becomes

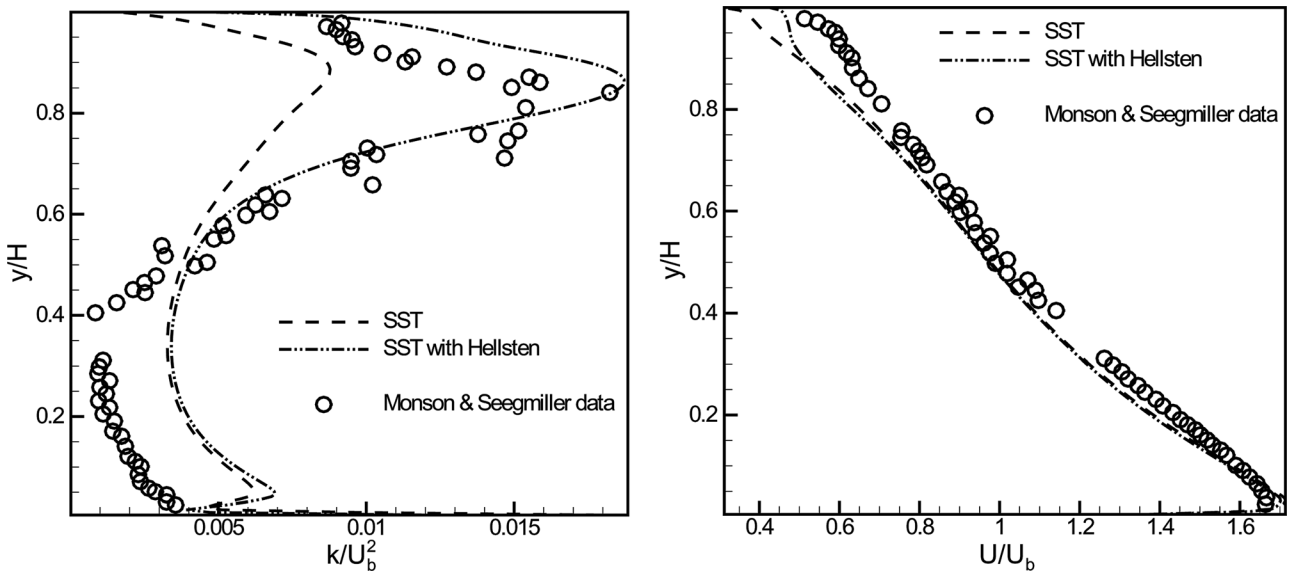

Fig. 7 Turbulent kinetic energy and mean velocity in a U-duct, in the middle of the bend. Dashed lines are the original SST model; chain-dashed lines invoke a curvature correction.

$$\mathbf{W} = \mathbf{\Omega}^S - \frac{3}{2}\left(\mathbf{\Omega}^S - \frac{\mathbf{S}^2 \cdot \mathbf{\Omega}^S + \mathbf{\Omega}^S \cdot \mathbf{S}^2}{|\mathbf{S}|^2}\right) \tag{40}$$

Any one of (38), (39) or (40) can be solved for $\mathbf{\Omega}^S$ given $\mathbf{W}$.

The convective derivative $D_t\mathbf{S} = \partial_t\mathbf{S} + \mathbf{U}\cdot\nabla\mathbf{S}$ involves the third order tensor $\partial_i\partial_j U_k$. Alternatively, a Lagrangian derivative

$$D_t\mathbf{S} \approx \frac{[\mathbf{S}(\mathbf{X}, t+\Delta t) - \mathbf{S}(\mathbf{x}, t)]}{\Delta t} \tag{41}$$

along the trajectory $d_t\mathbf{X} = \mathbf{U}(\mathbf{X}, t)$ starting at a computational node $\mathbf{X}(t) = \mathbf{x}$ and proceeding over one time-step, could be used. The rate of strain is interpolated from computational nodes to the endpoint $\mathbf{X}$. $\mathbf{W}$ can be evaluated by a centered formula as

$$\mathbf{W} = \frac{\mathbf{S}(\mathbf{x})\cdot\mathbf{S}(\mathbf{X}) - \mathbf{S}(\mathbf{X})\cdot\mathbf{S}(\mathbf{x})}{(|\mathbf{S}(\mathbf{X})^2 + |\mathbf{S}(\mathbf{x})|^2)\Delta t} \tag{42}$$

In a steady flow, Δt is arbitrary and could be selected so that the endpoint is on a cell boundary.

To show that $\mathbf{W}$ unifies system rotation and streamline curvature, consider the plane swirling flow $U_\theta(r)$. The angular velocity along curved streamlines is U_θ/r. The rate of strain tensor has the form

$$\mathbf{S} = S_{12}(r)[\mathbf{e}_1\mathbf{e}_2 + \mathbf{e}_2\mathbf{e}_1]$$

where $\mathbf{e}_1 = (\cos\theta, \sin\theta)$ and $\mathbf{e}_2 = (-\sin\theta, \cos\theta)$. Then with

$$D_t\mathbf{S} = \frac{U_\theta}{r}\partial_\theta\mathbf{S} = 2\frac{U_\theta}{r}S_{12}[\mathbf{e}_2\mathbf{e}_2 - \mathbf{e}_1\mathbf{e}_1]$$

and after calculating that $|\mathbf{S}|^2 = 2S_{12}^2$, one finds

$$\mathbf{W} = \frac{U_\theta}{r}[\mathbf{e}_1\mathbf{e}_2 - \mathbf{e}_2\mathbf{e}_1]$$

This has the form of a rotation tensor, with angular velocity U_θ/r. Thus, defining $\mathbf{W}$ in terms of the convective derivative unifies rotation and streamline curvature. It is *a fortiori* Galilean invariant, too.

Figure 7 is an example of the streamline curvature correction. The geometry is a U-shaped channel [see 32]. $y/H = 1$ is the outer, concave wall, next to which streamline curvature is destablizing. $y/H = 0$ is the inner, convex wall, which is stabilized by curvature. The profiles are at the middle of the U-bend, or 90 deg around the curve. The computations are with the SST version of k-ω, with and without Hellsten's curvature correction (21).

Acknowledgment

This work was funded in part by the National Science Foundation grant CBET-0965717.

References

[1] Rodi, W., and Scheurer, G., 1983, "Calculation of Curved Shear Layers With Two-Equation Turbulence Models," Phys. Fluids, **26**, pp. 1422–1436.
[2] Launder, B. E., Priddin, C. H., and Sharma, B. I., 1977, "The Calculation of Turbulent Boundary Layers on Spinning and Curved Surfaces," ASME Trans. J. Fluids Eng., **99**, p. 231.
[3] Durbin, P., and Pettersson Reif, B., 2010, *Statistical Theory and Modeling for Turbulent Flows*, 2nd ed., John Wiley and Sons, New York.
[4] Brethouwer, G., 2005, "The Effect of Rotation on Rapidly Sheared Homogeneous Turbulence and Passive Scalar Transport: Linear Theory and Direct Numerical Simulation," J. Fluid Mech., **542**, pp. 305–342.
[5] Kristoffersen, R., and Andersson, H. I., 1993, "Direct Simulations of Low-Reynolds-Number Turbulent Flow in a Rotating Channel," J. Fluid Mech., **256**, pp. 163–197.
[6] Lamballais, E., Metais, O., and Lesieur, M., 1998, "Spectral-Dynamic Model for Large-Eddy Simulations of Turbulent Rotating Channel Flow," Theor. Comput. Fluid Dyn., **12**, pp. 149–177.
[7] Grundestam, O., Wallin, S., and Johansson, A. V., 2008, "Direct Numerical Simulations of Rotating Turbulent Channel Flow," J. Fluid Mech., **598**, pp. 177–199.
[8] Iacovides, H., Launder, B. E., and Li, H. Y., 1996, "The Computation of Flow Development Through Stationary and Rotating U-Ducts of Strong Curvature," Int. J. Heat Fluid Flow, **17**, pp. 22–33.
[9] Witt, H. T., and Joubert, P. N., 1985, "Effect of Rotation on a Turbulent Wake," *Turbulent Shear Flows V*, Springer-Verlag, Berlin, pp. 21–25.
[10] Johnston, J. P., 1998, "Effects of System Rotation on Turbulence Structure: A Review Relevant to Turbomachinery Flows," Int. J. Rotating Mach., **4**, pp. 97–112.
[11] Barri, M., Khoury, G. K. E., Andersson, H. I., and Pettersen, B., 2009, "Massive Separation in Totating Turbulent Flows," *Advances in Turbulence XII*, B. Eckhardt, ed., Vol. 132, Springer, Berlin, pp. 625–628.
[12] Laskowski, G. M., and Durbin, P. A., 2007, "Direct Numerical Simulations of Turbulent Flow Through a Stationary and Rotating Infinite Serpentine Passage," Phys. Fluids, **19**, pp. 1–14.
[13] Andersson, H. I., 2010, "Effect of System Rotation on Free Shear Flows," *Effect of System on Turbulence With Application to Turbomachinery*, Von Karman Institute, Belgium, LS 2010–08.

[14] Speziale, C. G., and MacGiollaMhuiris, N., 1989, "On the Prediction of Equilibrium States in Homogeneous Turbulence," J. Fluid Mech., **209**, pp. 591–615.
[15] Piomelli, U., 1999, "Large-Eddy Simulation: Achievements and Challenges," Prog. Aerosp. Sci., **35**, pp. 335–362.
[16] Gatski, T. B., and Jongen, T., 2000, "Nonlinear Eddy Viscosity and Algebraic Stress Models for Solving Complex Turbulent Flows," Prog. Aerosp. Sci., **36**, pp. 655–682.
[17] Speziale, C. G., Sarkar, S., and Gatski, T. B., 1991, "Modelling the Pressure-Strain Correlation of Turbulence: An Invariant Dynamical Systems Approach," J. Fluid Mech., **227**, pp. 245–272.
[18] Bradshaw, P., 1973, "Effects of Streamline curvature on Turbulent Flow," AGARDograph, **169**.
[19] Hellsten, A., 1998, "Some Improvements in Menter's k-ω SST Turbulence Model," AIAA Paper No. 98-2554.
[20] Cazalbou, J., Chassaing, P., Dufour, G., and Carbonneau, X., 2005, "Two-Equation Modeling of Turbulent Rotating Flows," Phys. Fluids, **17**, pp. 1–14.
[21] Howard, J. Patankar, S. and Bordynuik, R., 1980. "Flow Prediction in Rotating Ducts Using Coriolis-Modified Turbulence Models," J. Fluids Eng., **102**, pp. 456–461.
[22] Pettersson-Reif, B. A., Durbin, P. A., and Ooi, A., 1999. "Modeling Rotational Effects in Eddy-Viscosity Closures," Int. J. Heat Fluid Flow, **20**, pp. 563–573.
[23] Park, J. Y., and Chung, M. K., 1999, "A Model for the Decay of Rotating Homogeneous Turbulence," Phys. Fluids, **11**, pp. 1544–1549.
[24] Thiele, M., and Müller, W.-C., 2009, "Structure and Decay of Rotating Homogeneous Turbulence," J. Fluid Mech., **637**, pp. 425–442.
[25] Spalart, P. R., and Shur, M. L., 1997, "On the Sensitization of Turbulence Models to Rotation and Curvature," Aerosp. Sci. Technol., **1**, pp. 297–302.
[26] Shur, M. L., Strelets, M. K., Travin, A. K., and Spalart, P. R., 2000, "Turbulence Modeling in Rotating and Curved Channels: Assessing the Spalart-Shur Correction," AIAA J., **38**, pp. 784–792.
[27] Khodak, A., and Hirsch, C., 1996, "Second Order Nonlinear Models With Explicit Effect of Curvature and Rotation," *Proceedings of the Third ECCOMAS Computational Fluid Dynamics Conference*.
[28] Dhakal, T. P., and Walters, K. D., 2011, "A Three-Equation Variant of the k-ω Model Sensitized to Rotation and Curvature Effects," J. Fluids Eng., submitted.
[29] Duraisamy, K., and Iaccarino, G., 2005, "Curvature Correction and Application of the v2-f Turbulence Model to Tip Vortex Flows," *Annual Research Briefs*, Center for Turbulence Research, Stanford University.
[30] Durbin, P., and Pettersson Reif, B., 1999, "On Algebraic Second Moment Models," Flow, Turbul. Combust., **63**, pp. 23–37.
[31] Girimaji, S., 1997, "A Galilean Invariant Explicit Algebraic Reynolds Stress Model for Turbulent Curved Flows," Phys. Fluids, **9**, pp. 1067–1077.
[32] Hellsten, A., 2002, "Curvature Corrections for Algebraic Reynolds Stress Modeling: A Discussion," AIAA J., **40**, pp. 1090–1911.
[33] Wallin, S., and Johansson, A., 2002, "Modelling Streamline Curvature Effects in Explicit Algebraic Reynolds Stress Turbulence Models," Int. J. Heat Fluid Flow, **23**, pp. 721–730.